ELSEVIER

Applied Surface Science 186 (2002) 150–155

applied surface science

www.elsevier.com/locate/apsusc

The early stage of the laser-induced oxidation of titanium substrates

L. Lavisse[a,*], D. Grevey[a], C. Langlade[b], B. Vannes[b]

[a]*LTm Lab., IUT du Creusot, 71200 Le Creusot, France*
[b]*IFoS Lab., STMS Dpt., Ecole Centrale de Lyon, BP 136, 69131 Ecully, France*

Abstract

Commercially pure titanium substrates have been treated using Q-switched Nd:YAG laser radiation ($\tau = 50$ ns, $\lambda = 1.06$ μm). The repetition of laser shots at the same location induces thermal cycling which leads to progressive oxidation and to the formation of multilayered coatings [1,2]. Previous studies have given us an overview of the various titanium oxides which could be formed as a function of the laser treatment parameters. This work focuses on the very early stage of the laser-induced oxidation, when the oxygen content does not exceed 50 at.% (TiO). The treated layers have been characterized by optical and SEM observation, EDS and X-ray diffraction analyses. The presence of the different new structures has been examined in relation with the Ti–O phase diagram. © 2002 Published by Elsevier Science B.V.

Keywords: Laser treatment; Oxidation; Phase diagram; Titanium

1. Introduction

Titanium and its alloys are mainly to be found in the aerospace field in which their high strength to density ratio are particularly attractive. However, their quite poor behavior in most of the encountered tribological situations, especially fretting, remains a limiting factor [1]. Numerous surface treatments have therefore been tested [3]. Among them, laser-assisted treatments, present particular interest as they allow the formation of non-equilibrium compounds on well localized areas [4]. Nitride [5] and carbide [6] have thus been formed on titanium samples under laser irradiation. Although continuous laser radiations have been mainly used in such kind of applications [5,7,8], pulsed lasers, having pulse duration in the nanosecond range, also lead to metallic surface treatment involving thermal effects [4,9–11]. By modifying the laser parameters, the global energy delivered on the surface may be varied, determining the kind of surface treatment (solid, liquid phase, etc.) that is achieved. The amount of diffused atoms in the treated surface is directly related to the repetition rate (i.e. number of pulses at the same surface location) [1,12]. However, the surface pretreatment (polishing, precoating, etc.) also has a great influence by modifying the diffusion kinetics as well as the absorption coefficient [5].

We report here the formation and characterization of oxide layers obtained by Nd:YAG laser surface treatment. The influence of the laser parameters and the environmental conditions have especially been investigated. The results are presented and commented with respect to the Ti–O equilibrium diagram.

* Corresponding author. Tel.: +33-385-424-319; fax: +33-385-424-329.
E-mail address: lavissel@iutlecreusot.u-bourgogne.fr (L. Lavisse).

0169-4332/02/$ – see front matter © 2002 Published by Elsevier Science B.V.
PII: S0169-4332(01)00761-9

Table 1
Titanium content (mol%)

Fe	<0.25
O	<0.15
C	<0.08
H	<0.0125
N	<0.06

2. Experimental

2.1. Titanium substrates

CP titanium (grade 4) substrates of dimension 15 mm × 10 mm × 1.2 mm were used (Table 1). Prior to oxidation, the sample surfaces were mechanically polished up to 1200 SiC grid before an electrolytic polishing in a perchloric acid with ethyleneglycol in methanol solution for 30 s at 24 V. The obtained target surfaces appear very smooth under SEM observation and do not present any anisotropic feature. X-ray diffraction and XPS analyses show that they are made of pure α-phase covered by a very thin (≈10 nm) layer of TiO_2-rutile.

2.2. Laser treatment

Treatments were carried out in air using a Nd:YAG radiation (1064 μm) from CHEVAL SA. Table 2 summarizes the different fixed laser parameters that have been used during this study. Using these conditions, the beam has a gaussian energy repartition and thermal effects are expected at the irradiated surface [4]. By varying the mean laser fluence in the range 2.5–25 J/cm^2, various colored layers may be formed on the target surface. In the following table, the results will be presented according to the obtained color.

2.3. Characterization

Surface and cross-section observations have been carried out by using optical and SEM microscopy. EDX analyses at 20 kV, using an Oxford JSM6400F FEG, have been performed and grazing incidence X-ray diffraction using the Cu Kα radiation at fixed incident angle in the range [0.5–8°], XPS and Auger using the Al Kα were also used to complete the surface characterization.

3. Results and discussion

3.1. Thermal field calculation

The existence of a liquid phase during the laser treatment has been confirmed by SEM observations. Numerical calculations seem to indicate that the melting temperature is reached 20 ns after the laser pulse beginning (using the parameters in Table 2) and the melting pool is about 2 μm thick, that corresponds to the thermal diffusion length [9,11]. In some cases, titanium vapor may also been created under irradiation as $T_{vTi} = 3600$ K. Emission spectroscopy spectrums prove this fact. Fig. 1 shows the evolution of the calculated maximal surface temperature as a function of time and sample depth.

The target is therefore submitted to a very abrupt heating and cooling rate of about 3×10^6 K s^{-1} leading to non-equilibrium phenomena [13,14]. As the thermal flux propagates underneath, the titanium substrate may first undergo the $\alpha \leftrightarrow \beta$ structural transformation prior to the β quenching under cooling. Raising the laser fluence increases the melted zone as well as the heat-affected depth in the titanium substrate.

3.2. Surface morphologies

The treated surfaces are characterized by linear, parallel scares due to the laser scanning. The distance between two consecutive lines (≈100 μm), corresponds to the laser beam diameter. The evolution in surface roughness confirms that the target surface has

Table 2
Laser parameters

Wavelength	Pulse duration	Pulse frequency	Displacement speed	Beam diameter	Distance between two consecutive lines
1.064 mm	50 ns	5 kHz	50 mm s^{-1}	100 μm	20 μm

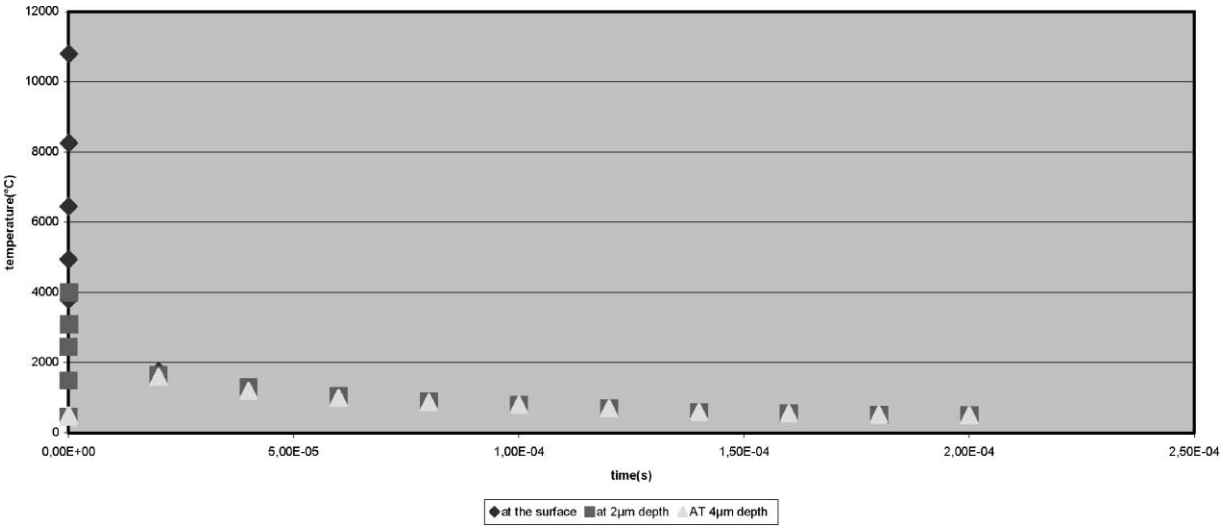

Fig. 1. Temperature evolution, at different depths during one period, on titanium target irradiated at 2.5 J/cm^2, 5 kHz and 50 mm/s.

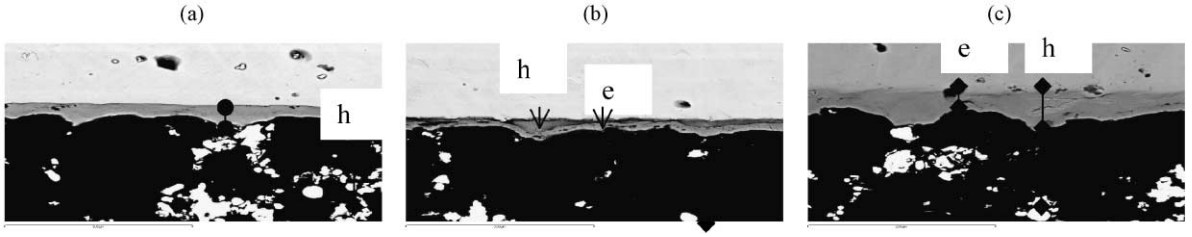

Fig. 2. SEM observations on profile oxide layers after laser irradiation with the EDS analyze for the oxygen composition—(a) uncolored layers: $h = 15\,\mu m$, $e = 6\,\mu m$, $x_{mol}(O) = 0.30$; (b) yellow layers: $h = 13.5\,\mu m$, $e = 6\,\mu m$, $x_{mol}(O) = 0.37$; (c) purple layers: $h = 27\,\mu m$, $e = 10\,\mu m$, $x_{mol}(O) = 0.33$.

been heated up to the liquid phase. More surprising is the formation of a colored layer (Fig. 2). Cross-section observations reveal that these layers are less than 5 μm thick for the colorless and yellow films and about 10 μm thick for the purple coating (Fig. 2). Such thicknesses and the very abrupt color evolution (threshold effect) clearly show that the observed color cannot be related to optical interference effects [1] (Fig. 3).

3.3. Structural analyses

Even if the equilibrium hypotheses are not fulfilled during pulsed laser treatment, binary phase diagram can successfully be used to understand the formation or absence of the various compounds [5,15]. As several Ti–O diagrams may be found in literature [16], we choose to base our discussion on the most

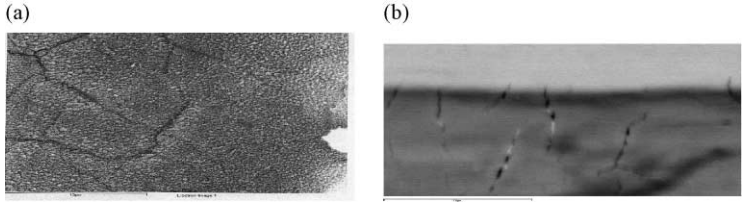

Fig. 3. Details with SEM observations (5000×): (a) at the bottom of a purple layer; (b) on the profile of an uncolored layer.

complete which mixed calculated and experimental results [17] (Fig. 1).

3.3.1. Colorless and yellow layers

GIRXD analyses performed at incidence angle ranging from 0.5° to 8° on these layers reveal the presence of oxygen-rich compounds at the sample surface (Table 4). For the highest incident angles, the longer X-ray beam penetration enables the subsurface characterization. It is made of a mixture of several hexagonal compounds, i.e. Ti_6O, Ti_3O and Ti_2O (oxygen ordering in the hexagonal α-Ti structure). Their presence may easily be explained by the oxygen diffusion through the melted treated surface to the bulk material. However, the *c* lattice parameters experimentally observed in our Ti_6O and Ti_3O structure are much larger than the one of the α-Ti initial lattice. If this effect has already been reported for thermal oxidation of titanium [17,18], its very large amplitude is likely to be related to the laser irradiation specificity. In case of a CO_2 laser treatment, previous studies revealed the anisotropic oxygen diffusion [19]. At lower incidence angles, the main product has been identified as TiO_x. XPS analyses confirm the presence of Ti(II) species as well as the presence of a TiO_2 thin layer at the very extreme surface (Table 3).

However, some differences exist between the colorless and yellow layers. First the Ti_6O structure, observed in the colorless sample has not been detected in the yellow one using the same diffraction conditions (Table 4). As the later samples have been obtained at higher laser fluences, the oxygen diffusion length is likely to be longer, so the Ti_6O structure should appear at a greater depth, that is not accessible under our diffraction conditions. Secondly, the amount of Ti(II) species detected using XPS analysis is about three times larger on the yellow layer than on the colorless sample and the observed quantity of oxygen, as detected by EDX analysis, is also much larger in the case of the yellow surface (Tables 3 and 4). Moreover, a greater discrepancy exists in the oxygen content between the outermost oxide layers and the underneath oxygen-rich titanium. These effects can be explained by considering the Ti–O phase diagram. In the case of the colorless surface, the mean oxygen atomic composition of 0.33, which may be written as Ti_2O, slightly excesses the high temperature (1905 °C) congruently oxide composition. Therefore, the oxygen-rich melted pool would likely to solidify according to the 1767 °C equilibrium [16] leading to the formation of the Ti_2O hexagonal form and TiO_x ($x = 0.42$ at.% here) (Fig. 4). The colorless sample, having a lower oxygen content at the surface, will precipitate less TiO_x than the other samples, treated at higher fluences and having trapped more oxygen in the liquid phase. Knowing that the particular electronic structure of TiO_x leads to a characteristic yellow color, the observed color effect is consistent with the Ti–O phase diagram and the various performed analyses [20].

Table 3
Oxidation states of titanium and oxygen identify with XPS and Auger analyses

Oxidation states (%)	Ti(+II)	Ti(+III)	Ti(+IV)	O(−II)	$O(OH^-)$	*R*
Reference	5	5	90	65	35	0.50
Colorless	5	25	70	90	10	0.70
Yellow	15	20	65	80	20	0.74
Purple	5	20	75	85	15	0.50

3.3.2. Purple layers

The GIXRD and XPS analyses confirm the results presented above, the amount of diffused oxygen and its diffusion length being larger. The oxygen content in the subsurface titanium remains constant at about 30 at.% and the XRD spectra show the presence of the ordered hexagonal phases. In the outermost layers, the oxygen content reaches values as high as 0.57 at.%

Table 4
Characterized phases with GIXRD analyses

Layers	*θ*–2*θ*	8°	1°
Reference	Ti(α)	Ti(α)	
Colorless	Ti(α), $Ti_2O_{(hcc)}$, TiO_{cfc}	Ti(α), $Ti_2O_{(hcc)}$, TiO_{cfc}	à 0.5°, Ti(α), $Ti_3O_{(hcc)}$, $Ti_2O_{(hcc)}$, TiO_{cfc}, $TiO_{2(t)}$
Yellow	Ti(α), $Ti_2O_{(hcc)}$, TiO_{cfc}	Ti(α), $Ti_3O_{(hcc)}$, $Ti_2O_{(hcc)}$, TiO_{cfc}	Ti(α), $Ti_3O_{(hcc)}$, $Ti_2O_{(hcc)}$, deux phases, TiO_{cfc}
Purple	Ti(α), $Ti_2O_{(hcc)}$, $Ti_3O_{(hcc)}$, TiO_{cfc}	Ti(α), $Ti_2O_{(hcc)}$, $Ti_3O_{(hcc)}$, $TiO_{(cfc)}$	Ti(α), $Ti_2O_{(hcc)}$, $Ti_3O_{(hcc)}$, TiO_{cfc}, $Ti_2O_{3(hcc)}$, $TiO_{2(m)}$

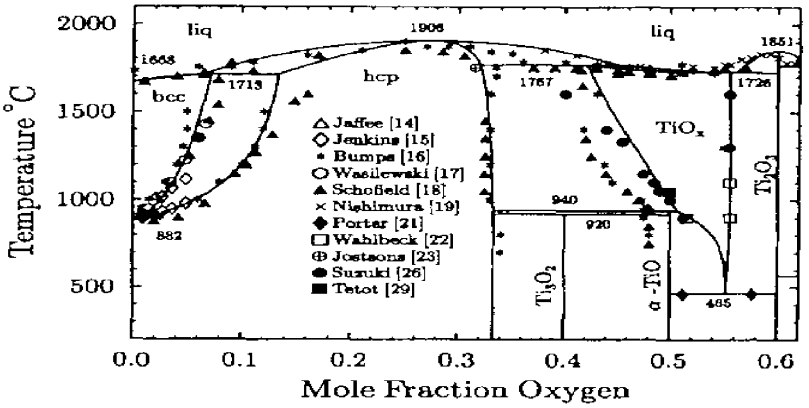

Fig. 4. Ti–O system phase diagram for a content in mole fraction of oxygen less than 0.62 (Waldner).

and Ti(III) and Ti(IV) species are observed. GIRXD reveals the presence of a new variety of oxide, i.e. Ti_2O_3. Considering the Ti–O phase diagram, the tiny composition range allowed for Ti_2O_3 ($O/Ti = 1.49-1.51$) and the observed oxygen content in our sample and the absence of Ti_3O_5 compound, the congruent melting at 1851 °C should be excluded. A solidification path through the liquid $\Leftrightarrow$ TiO_x+ Ti_2O_3 equilibrium at 1726 °C is in good accordance with the observed results. The deduced oxygen ratio in the TiO_x phase should therefore be 0.6 and the identified hexagonal Ti_2O_3 phase has a lattice parameter $a = 0.5139$ nm ($c = 1.3659$ nm) very similar to the value $a = 0.515$ nm given by other authors ($c = 1.36$ nm) [16]. If most of the identified compound may be explained with the help of the Ti–O phase diagram, some results are still to be clarified. The absence of α-TiO is particularly noticeable. This structure is the low temperature stoichiometric modification of the high temperature TiO_x solid solution and should therefore be observed instead of the identified TiO_x. In fact the $TiO_x \rightarrow$ α-TiO transformation is a vacancies ordering phenomenon [20] which is likely to be inhibited due to the specific cooling conditions. In the case of the TiO_2 very thin upper layer that has a unusual monoclinic structure, no explanation has yet been found.

4. Conclusions

The early stage of the laser assisted oxidation of titanium surface in ambient atmosphere has been studied, the produced compounds have been identified and their formation has been explained based on the Ti–O phase diagram. To summarize:

- The thermal effects, induced by the pulsed laser irradiation, lead to the formation of a melted pool whose thickness depends on the laser fluence whatever the repetition rate be.
- Due to the oxygen diffusion in the irradiated target, oxygen-rich phases are formed. The observed oxides found in the melted zone are consistent with the high temperature structures of the Ti–O phase diagram. The cooling rate during the laser treatment is high enough to quench them.
- In the heat-affected zone, the oxygen diffusion leads to the formation of the ordered Ti_6O, Ti_3O, Ti_2O structure, having anomalous lattice parameters.
- The α-TiO oxide has not been identified in any of the laser treated sample. It should have been formed under cooling from the liquid phase or also as a result of the oxygen diffusion in the heated but not melted titanium substrate.

Further work is in progress to explore the rest of the phase diagram, corresponding to higher fluence-laser treatments. Irradiation tests under vacuum and controlled atmosphere are also planned.

Acknowledgements

LL thanks N. Guigue-Millot (LRRS University of Dijon) for his help in X-ray analysis.

References

[1] C. Langlade, A.B. Vannes, J.M. Krafft, J.R. Martin, Surf. Coat. Technol. 100–101 (1998) 383.
[2] L. JungChang, C. Langlade, A.B. Vannes, Surf. Coat. Technol. 115 (1997) 87.
[3] P. Guiraldenq, Matériaux et techniques (1987) 487.
[4] D. Bauerle, Laser Processing and Chemistry, 2nd Edition, Springer, Berlin, 1996, p. 6T.
[5] P. Laurens, H. L'Enfant, M.C. Sainte Catherine, J.J. Bléchet, J. Amouroux, Thin Solid Films 293 (1997) 220.
[6] B. Courant, J.J. Hantzpergue, S. Benayou, Wear 236 (1999) 39.
[7] D.A. Jelski, L. Nanai, R. Vajtai, I. Hevesi, T.F. Georges, Mater. Sci. Eng. A 173 (1993) 193.
[8] L. Nanai, I. Hevesi, R. Vajtai, D. Jelski, T.F. Georges, Thin Solid Films 227 (1993) 13.
[9] J.V. Daurelle, T. Sarnett, M. Autric, Lasers Eng. 8 (3) (1999) 185.
[10] L. Nanai, R. Vajtai, T.F. Georges, Thin Solid Films 298 (1997) 160.
[11] A. Ougazzaden, L. Silvestre, A. Mircea, N. Bouadma, G. Patriarche, M. Juhel, Proceedings of the International Conference on Indium Phosphide and Related Materials, 1997, p. 598.
[12] E. Sicard, C. Boulmer-Leborgne, T. Sauvage, Appl. Surf. Sci. 127–129 (1998) 726.
[13] R. Vajtai, C. Beleznai, L. Nanai, Z. Gingl, T.F. George, Appl. Surf. Sci. 106 (1996) 247.
[14] L. Nanai, R. Vajtai, T.F. Georges, Thin Solid Films 298 (1997) 160.
[15] A.I. Nwobu, R.D. Rawlings, D.R.F. West, Acta Mater. 47 (2) (1999) 631.
[16] A.D. Mac Quillan, M.K. Mac Quillan, Titanium, Butterworths, London, 1956, pp. 246–253.
[17] P. Waldner, P. Eriksson, Calphad 23 (2) (1999) 189.
[18] M.L. Walsh, F.R. Brotzen, R.B. Mac Lellan, A.J. Griffin, Int. Mater. Rev. 41 (1) (1996) 1.
[19] N.G. Evtushenko, S.G. Kostyuk, A.A. Mal'gota, C. Von Men, M.N. Chesnokov, Khimiiya Obrabotki Materialov 21 (1) (1987) 49.
[20] L. Smart, E. Moore, Solid State Chemistry: An Introduction, 2nd Edition, Chapman & Hall, London, 1995, p. 108.